Available online at www.sciencedirect.com
ScienceDirect
Journal of the European Ceramic Society 32 (2012) 1413–1417
www.elsevier.com/locate/jeurceramsoc

Fabrication of Si_3N_4-based composite containing needle-like TiN synthesized using NH_3 nitridation of TiO_2 nanofiber

Hajime Kiyono [a,*], Yuho Miyake [a], Yusuke Nihei [a], Tomoki Tumura [b], Shiro Shimada [a]

[a] *Faculty of Engineering, Hokkaido University, Kita-ku, Sapporo 060-8628, Japan*
[b] *Faculty of Engineering, Oita University, Dannoharu, Oita 870-1192, Japan*

Available online 4 May 2011

Abstract

A Si_3N_4 composite containing needle-like TiN particles (7 vol%) was fabricated. Needle-like TiN particles several micrometers long were synthesized using NH_3 nitridation of TiO_2 nanofiber, which was obtained using hydrothermal treatment. A mixed powder of α-Si_3N_4 and the needle-like TiN particles with additives was hot pressed at 24 MPa and 1850 °C for 1 h in N_2 atmosphere. Mechanical properties of the composite were compared with those of a composite containing rounded TiN particles and a monolithic β-Si_3N_4 ceramic. The Si_3N_4 matrix of the composites containing TiN was mainly *a*-phase, suggesting that the α–β phase transformation of Si_3N_4 was inhibited by the presence of TiN. Although fracture strength of the composites was lower, fracture toughness was comparable to that of monolithic β-Si_3N_4 ceramics. Hardness of the composites was about 19 GPa and was greater than that of the monolithic β-Si_3N_4 ceramic.

Keywords: Composite; Titanium nitride; Silicon nitride; Needle; Nanofiber; Hot pressing

1. Introduction

TiN is a promising material for coatings or additives in composites because of its high hardness characteristic, high fracture toughness, good abrasive resistance, good adhesive properties, and high electron conductivity. Fabrication of TiN–Si_3N_4 composites has been reported to give electric conductivity or to improve fracture toughness.[1–4] In these reports, the size of TiN particles has been controlled to the micrometer[2,3] or nanometer[4] range but the shape has not been intentionally controlled. It is well known that introducing needle-like grains into a ceramic body improves fracture toughness by virtue of a deflection and bridging effect against a crack propagating. Fibers or whiskers of TiN have been synthesized using methods, such as chemical vapor deposition,[5] nitridation of TiO_2 fibers,[6] and carbothermal reduction of TiO_2 with additions.[7] It is known that TiO_2 is easily nitrided to TiN using NH_3 atmosphere at elevated temperatures according to the following reaction:

$$2TiO_2 + 2NH_3 \rightarrow 2TiN + 3H_2O + 1/2O_2. \quad (1)$$

TiO_2 nanofibers with large specific surface area can be obtained by using the hydrothermal treatment of TiO_2 powder in a basic solution.[8,9] The authors have recently demonstrated that partially nitrided nanofiber has high rate charge-discharge properties can be used as an electrode material for lithium ion batteries.[10] In the study, we found that the nitrided nanofiber possesses a needle-like shape several μm long, which originates from the nanofiber. However, nitridation conditions and other applications of the nitrided nanofiber have not been investigated. In the present paper, we investigate the nitridation conditions necessary to synthesize needle-like TiN particles by the nitridation of TiO_2 nanofibers and fabricate Si_3N_4-based composites containing the needle-like TiN particles.

2. Experimental procedures

2.1. Synthesis of needle-like TiN particles

TiO_2 nanofibers were synthesized by hydrothermal treatment of TiO_2 powder[8,11] using rutile TiO_2 powder (CR-EL, 0.3 μm; Ishihara Industry Co., Japan). The dispersion of 10 wt% TiO_2 powder in 47 wt% KOH and 43 wt% H_2O was heated at 150 °C for 150 h in a stainless jacket lined with TEFLON. The powder was then washed with 0.1 mol/L HCl solution to remove

* Corresponding author. Tel.: +81 11 706 6578; fax: +81 11 706 6578.
E-mail address: kiyono@eng.hokudai.ac.jp (H. Kiyono).

0955-2219/$ – see front matter © 2011 Elsevier Ltd. All rights reserved.
doi:10.1016/j.jeurceramsoc.2011.04.008

potassium and dried. To determine the nitridation conditions needed to transform TiO_2 nanofibers to TiN, thermogravimetric analysis (TGA) in NH_3/Ar atmosphere was carried out. Details of the TGA equipment are described elsewhere.[12] About 50 mg of the TiO_2 nanofibers was heated to 1200 °C at 5 °C/min in NH_3/Ar (50/50 kPa). The weight loss during heating was monitored by an electric balance (Cahn D-200, USA). Nitridation was also carried out using a horizontal tube furnace using the same conditions as that of TGA except for the amount of the sample, which was about 0.5 g. The heat-treated samples were then subjected to X-ray diffraction (XRD, RIGAKU RINT, Japan) analysis, transmission electron microscopic (TEM, JEOL JEM-2000FX, Japan) observation, and X-ray photo electron spectroscopic (XPS, SHIMADZU ESCA-750, Japan) analysis.

2.2. Fabrication and characterization of composites

α-Si_3N_4 (SN-E10, Ube industry Co., Japan), Y_2O_3 (Koujyundo Chemical Co., Japan), and Al_2O_3 (Kanto Chemical Co., Japan) powders were used. The powders of α-Si_3N_4 with 5 wt% Y_2O_3 and 5 wt% Al_2O_3 were mixed using a ball mill containing plastic-coated iron balls in ethanol. After the 24 h ball milling, a dispersion of the TiO_2 nanofibers in water was added to the mixed powder of α-Si_3N_4 with Y_2O_3 and Al_2O_3 in ethanol and was mixed for 1 h. The amount of added TiO_2 nanofiber corresponds to 7 vol% TiN in the fabricated composites. The mixed powder was dried and heated using a horizontal tube furnace in NH_3 atmosphere at 1000 °C for 4 h to transform TiO_2 to TiN without the nitridation of Al_2O_3 and Y_2O_3. The heated powder was hot pressed under a uniaxial pressure of 24 MPa at 1850 °C for 1 h in N_2 atmosphere (Composite A). For comparison, a TiN–Si_3N_4 composite having the same composition as that of Composite A, but with TiN fabricated from TiO_2 (CR-EL) powder without hydrothermal treatment, (Composite B) and a monolithic Si_3N_4 ceramic were fabricated. Hot pressing conditions for Composite B and the monolithic Si_3N_4 were the same as those of Composite A. The composites and monolithic Si_3N_4 were characterized by XRD and scanning electron microscope (SEM, JEOL JSM-6300F, Japan). Fracture strength was determined using a four-point bending test with a crosshead speed of 0.05 mm/min. Fracture toughness and hardness were measured using Vickers indentation method at an applied pressure of 195 and 49 N, respectively.

3. Results and discussion

3.1. Nitridation of TiO_2 nanofibers

Fig. 1 shows non-isothermal TGA curves of as-received TiO_2 powder (CR-EL) and TiO_2 nanofibers in NH_3/Ar (50/50 kPa). The weight of the as-received TiO_2 powder started to decrease from about 720 °C but the slope of the weight loss curve decreased at 870 °C. At about 1100 °C, the weight loss stopped at about 21%, which was close to the theoretical weight loss of 22.5% based on Eq. (1). Using XRD analysis, it was found that the sample was transformed to TiN after the TGA. Based on the results of TGA and XRD analysis, nitridation of as-received TiO_2 powder started at 720 °C and the powder was completely nitrided at 1100 °C in NH_3/Ar atmosphere. However, the weight of TiO_2 nanofibers started to decrease at room temperature, reaching a plateau at temperatures between 400 and 720 °C. After the plateau, the weight decreased again to 30% at 1030 °C, showing no significant change above that temperature.

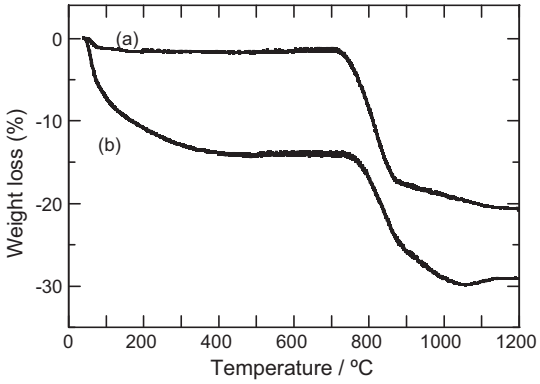

Fig. 1. TGA results of (a) as-received TiO_2 and (b) TiO_2 nanofibers in NH_3/Ar (50/50 kPa) atmosphere with a heating rate of 5 °C/min.

XRD patterns of the TiO_2 nanofibers heated to various temperatures using the horizontal tube furnace are shown in Fig. 2. The original pattern of TiO_2 nanofibers showed small and broad peaks corresponding to those of $H_2Ti_3O_7$.[13] The sample heated to 800 °C showed definitive peaks of anatase, indicating that the original TiO_2 nanofibers were dehydrated and crystallized. The TGA analysis showed that the first weight loss was about 20%, which was less than the estimated value of 7.0%, calculated from the equation:

$$H_2Ti_3O_7 \rightarrow 3TiO_2 + H_2O. \quad (2)$$

The observed greater weight loss suggests that the nanofibers contained a large amount of physically adsorbed H_2O or the presence of hydrated species other than $H_2Ti_3O_7$. The XRD pattern of the sample heated up to 900 °C showed small peaks of rutile

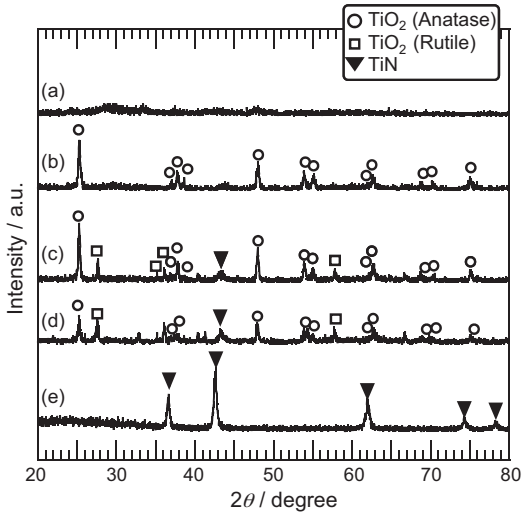

Fig. 2. XRD patterns of (a) as-synthesized TiO_2 nanofibers and ones heated at (b) 800 °C, (c) 900 °C, and (d) 1000 °C with no holding time and (e) at 1000 °C for 1 h in NH_3/Ar (50/50 kPa).

Table 1
Results of XPS and XRD analysis of TiO_2 nanofibers heated to various temperatures in NH_3 atmosphere.

Temperature	N/Ti (%)	Phases observed by XRD
800	0	Anatase
850	2	Anatase ⋙ rutile, TiN
900	4	Anatase ≫ rutile, TiN
950	20	Anatase > rutile, TiN

and TiN, in addition to the peaks of anatase. The pattern of the 1000 °C sample showed that the peak intensity of TiN and rutile increased. The sample heated at 1000 °C for 1 h showed only peaks of TiN with a lattice constant of $a = 0.423$ nm, which is in close agreement with the reported TiN value of 0.4238.[14] Table 1 summarizes the XRD and XPS results for the heat-treated samples. It was found that the concentration of nitrogen increased with increasing temperature.

Fig. 3 shows the TEM photographs of as-synthesized and heat-treated TiO_2 nanofibers at 800–1000 °C. As-synthesized TiO_2 nanofibers (Fig. 3(a)) showed a fibrous shape and the larger ones were 2–5 mm long and 100 nm wide. The heat-treated sample at 800 °C (Fig. 3(b)) retained its fibrous shape but the fibers became shorter and changed to aggregates of small grains. (some of the grains are indicated by arrows). The length of the needle-like grains became short with increasing of the temperature from 900 to 1000 °C (Fig. 3(c) and (d)). However, in the sample heated at 1000 °C for 1 h (Fig. 3(e)), the grains sintered together while retaining a fibrous shape. From the highly magnified image (Fig. 3(e′)), it was found that the crystallites were well sintered together and the boundaries between crystallites decreased comparing with the sample heated at 1000 °C with no holding time (Fig. 3(d)), expecting that the sample heated at 1000 °C for 1 h has high tensile strength.

3.2. Fabrication and mechanical properties of composites

Fig. 4 shows the XRD patterns of Composite A (containing needle-like TiN particles), Composite B (rounded TiN particle), and the Si_3N_4-sintered body by hot-pressing at 1850 °C for 1 h in N_2 atmosphere. All the samples had relative densities of 96–98%. It was found that Composite A consisted of α-Si_3N_4 and TiN with a small amount of β-Si_3N_4. Composite B showed an XRD pattern similar to that of Composite A, but the peaks of β-Si_3N_4 were slightly higher than those in the pattern of Composite A. On the other hand, monolithic Si_3N_4 consisted mostly of β-Si_3N_4 with a small amount of α-Si_3N_4. In general, sintering of Si_3N_4 ceramic occurs through a process in which an intergranular liquid phase is formed by additives and SiO_2, present in the Si_3N_4 powder (liquid phase sintering), resulting in a sintered body consisting mainly of β-Si_3N_4.[15] Although it was reported that an α-Si_3N_4 ceramic body was fabricated by spark plasma sintering to shorten the sintering time,[16] it is difficult to obtain α-Si_3N_4 ceramic using conventional methods, such as hot pressing, hot isostatic pressing, and pressureless sintering. Results of the present study (Table 2) indicate that the presence of TiN particles inhibits the transformation to β-Si_3N_4 but the mechanism

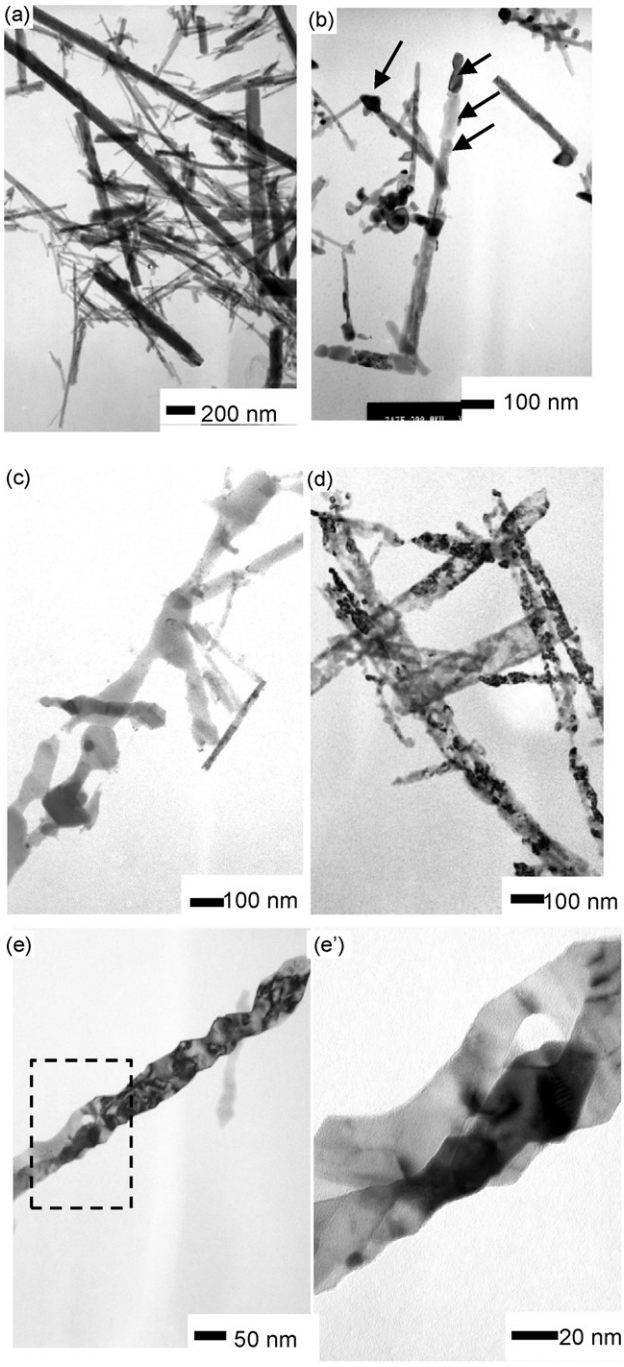

Fig. 3. TEM photographs of TiO_2 nanofibers and nitrided ones. Photos (a) through (e) are same as those in Fig. 2, and (e′) is a magnified image of (e). Arrows in (b) shows the grains consisting of needle-like particles.

inhibiting the transformation is not clear. Fig. 5 shows SEM photographs of the polished and fracture surface of Composite A. In the polished surface image, TiN particles, shown as gray parts, were dispersed in the composites but some agglomerations several nanometers in size were observed. At the fracture surface, needle-like TiN particles were observed (Fig. 5(b)), showing that TiN particles maintained the needle shape during sintering.

Fig. 6 shows the plots of fracture strength, toughness, and hardness of the samples. The fracture strengths of the Composites A and B are about 230 and 350 MPa, respectively, and are

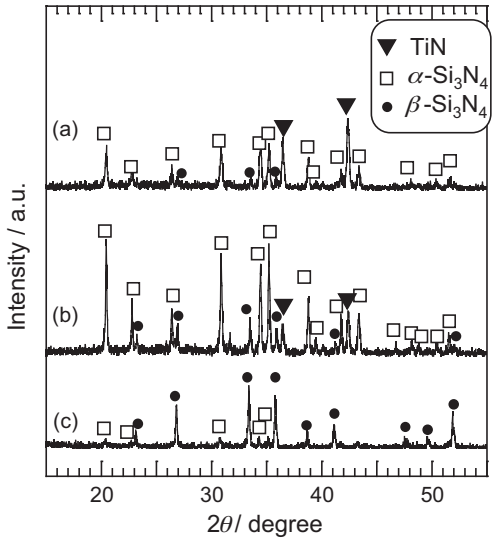

Fig. 4. XRD patterns of (a) Composites A and (b) B, and (c) Si_3N_4.

less than that of the reference sample of monolithic Si_3N_4. The reported fracture strength of α-Si_3N_4 is 300–420 MPa,[16] which is less than the typical value of β-phase (600–800 MPa). The low strength of Composites A and B is because the matrices of the composites are primarily composed of α-Si_3N_4. Fracture toughness of Composite A (needle-like TiN) was equivalent to that of monolithic Si_3N_4, taking into consideration the scattering of the value. There was no remarkable improvement in the fracture toughness of Composite A as compared to that of Composite B, possibly because of the presence of agglomerations of TiN. Hardness of Composite A improved in comparison to that of both Composite B and monolithic Si_3N_4, showing that the needle-like TiN effectively improved the hardness.

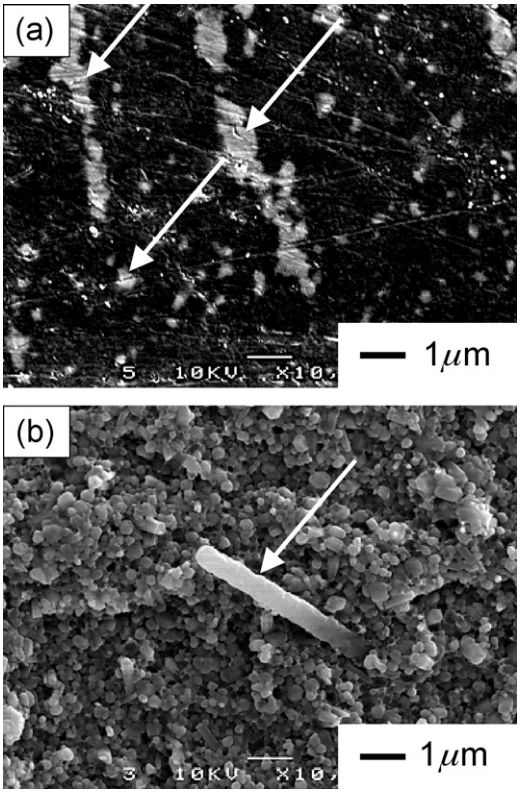

Fig. 5. SEM photographs of (a) polished and (b) fracture surface of Composite A. Arrows in photographs denote TiN grains.

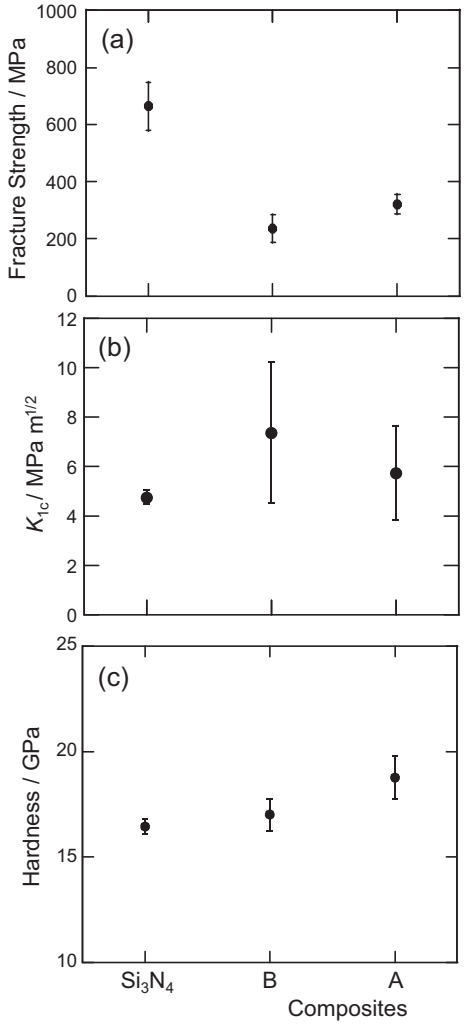

Fig. 6. Plots of (a) fracture strength, (b) fracture toughness, and (c) the Vickers hardness of the Composites A and B and monolithic Si_3N_4. Error bars show standard deviation.

Table 2
Composition and observed phases of sintered samples.

Sample	TiN (vol%)	Shape of TiN	Phases observed by XRD
Composite A	7	Needle like	TiN, α-$Si_3N_4 \gg \beta$-Si_3N_4
Composite B	7	Rounded	TiN, α-$Si_3N_4 \gg \beta$-Si_3N_4
Monolithic Si_3N_4	0	–	β-$Si_3N_4 \gg \alpha$-Si_3N_4

4. Summary

Si_3N_4 composites containing needle-like TiN particles were fabricated by hot pressing. The needle-like TiN powder was synthesized by NH_3 nitridation of TiO_2 nanofibers obtained by hydrothermal treatment. The obtained composites consisted of α-Si_3N_4 and TiN, with a small amount of β-Si_3N_4, suggest-

ing that the presence of TiN delays the phase transformation of Si_3N_4. Fracture strength of the composites was lesser than that of monolithic β-Si_3N_4 ceramic. However, fracture toughness was equivalent to that of monolithic β-Si_3N_4 ceramic and hardness improved in comparison to that of β-Si_3N_4.

Acknowledgments

This study was financially supported by GCOE program of Catalysis as the Basis for the Innovation in Materials Science (Hokkaido University) and Promoting Technological Seeds program of Research for Japan Science and Technology Agency (JST).

References

1. Bellosi A, Tampieri A, Liu YZ. Oxidation behavior of electroconductive Si_3N_4–TiN composites. *Mater Sci Eng A* 1990;**127**(1):115–22.
2. Bellosi A, Guicciardi S, Tampieri A. Development and characterization of electroconductive Si_3N_4–TiN composites. *J Eur Ceram Soc* 1992;**9**:83–92.
3. Tatami J, Chen IW, Yamamoto Y, Komastu M, Komeya K, Kim DK, Wakihara T, Meguro T. Fracture resistance and contact damage of TiN particle reinforced Si_3N_4 ceramics. *J Ceram Soc Jpn* 2006;**114**(1335):1049–53.
4. Kawano S, Takahashi J, Shimada S. Fabrication of TiN/Si_3N_4 ceramics by spark plasma sintering of Si_3N_4 particles coated with nanosized TiN prepared by controlled hydrolysis of Ti(O–i–C_3H_7). *J Am Ceram Soc* 2003;**86**(4):701–5.
5. Bojarski Z, Wokulska K, Wokulski Z. Growth morphology of titanium nitride whiskers. *J Cryst Growth* 1981;**52**(April):290–5.
6. Kamiya K, Yoko T, Bessho M. Nitridation of TiO_2 fibers prepared by the sol–gel method. *J Mater Sci* 1987;**22**(3):937–41.
7. Krishnarao RV, Subrahmanyam J, Yadagiri M. Formation of TiN whiskers through carbothermal reduction of TiO_2. *J Mater Sci* 2002;**37**(8):1693–9.
8. Kasuga T, Hiramatsu M, Hoson A, Sekino T, Niihara K. Formation of titanium oxide nanotube. *Langmuir* 1998;**14**(12):3160–3.
9. Kasuga T. Formation of titanium oxide nanotubes using chemical treatments and their characteristic properties. *Thin Solid Films* 2006;**496**(1):141–5.
10. Tanaike O, Kiyono H, Shimada S, Toyoda M, Tsumura T. Ammonia-treated titania as an anode material of lithium-ion battery with high-rate capability. *ECS Trans* 2009;**16**:151–6.
11. Yuan ZY, Su BL. Titanium oxide nanotubes, nanofibers and nanowires. *Colloids Surf Physicochem Eng Aspects* 2004;**241**(1–3):173–83.
12. Sakai T, Kiyono H, Shimada S. Kinetics and mechanism of formation of GaN from β-Ga_2O_3 by NH_3. *Mater Res Soc Symp Proc* 2009:1202–10.
13. ICDD 47-0561.
14. ICDD 87-0633.
15. Riley FL. Silicon nitride and related materials. *J Am Ceram Soc* 2000;**83**(2):245–65.
16. Chen F, Shen Q, Yan FQ, Zhang LM. Spark plasma sintering of alpha-Si_3N_4 ceramics with MgO–$AlPO_4$ as sintering additives. *Mater Chem Phys* 2008;**107**(1):67–71.